NEOPLASIA
www.neoplasia.com

Volume 18 Number 10 October 2016 pp. 610–617 610

p53 and *p16*^{Ink4a}/*p19*^{Arf} Loss Promotes Different Pancreatic Tumor Types from PyMT-Expressing Progenitor Cells[1,2]

Stephanie Azzopardi*, Sharon Pang*, David S. Klimstra† and Yi-Chieh Nancy Du*

*Department of Pathology and Laboratory Medicine, Weill Cornell Medicine, New York, NY 10065, USA; †Department of Pathology, Memorial Sloan Kettering Cancer Center, New York, NY 10065, USA

Abstract

In human studies and mouse models, the contributions of *p53* and *p16*^{Ink4a}/*p19*^{Arf} loss are well established in pancreatic ductal adenocarcinoma (PDAC). Although loss of functional p53 pathway and loss of *Ink4a/Arf* in human pancreatic acinar cell carcinoma (PACC) and pancreatic neuroendocrine tumor (PanNET) are identified, their direct roles in tumorigenesis of PACC and PanNET remain to be determined. Using transgenic mouse models expressing the viral oncogene *polyoma middle T antigen* (*PyMT*), we demonstrate that *p53* loss in pancreatic *Pdx1*+ progenitor cells results in aggressive PACC, whereas *Ink4a/Arf* loss results in PanNETs. Concurrent loss of *p53* and *Ink4a/Arf* resembles loss of *p53* alone, suggesting that *Ink4a/Arf* loss has no additive effect to PACC progression. Our results show that specific tumor suppressor genotypes provocatively influence the tumor biological phenotypes in pancreatic progenitor cells. Additionally, in a mouse model of β-cell hyperplasia, we demonstrate that *p53* and *Ink4a/Arf* play cooperative roles in constraining the progression of PanNETs.

Neoplasia (2016) 18, 610–617

Introduction

Pancreatic acinar cell carcinomas (PACCs) and pancreatic neuroendocrine tumors (PanNETs) are neoplasms that each account for 1% to 2% of pancreatic cancers in adults [1,2]. PACC has a 25% to 50% 5-year survival rate, whereas PanNET survival is 100% for low-stage cancers and drops to 55% for stage IV cancers [2–4]. Both PACCs and PanNETs have a tremendous amount of genomic instability at the nucleotide and chromosomal level [2,5–7]. Complicating clinical diagnosis, PACC can also present as mixed acinar-neuroendocrine carcinomas (neuroendocrine differentiation in >30% of tumor), mixed acinar-ductal carcinomas, or mixed with both neuroendocrine and ductal components [8]. Because of the availability of clinical PanNET and PACC specimens, studies have been limited, and the pathogenesis of both cancers is poorly understood.

Alterations in PDAC are well-defined and commonly include activating mutations in *KRAS* as the driver mutations and alterations in the tumor suppressors *p53* (50%-70% of cases) and *p16*^{Ink4a} (80%-95% of cases) [9]. The loss of *p53* and *p16*^{Ink4a} in PDAC suggests important, nonredundant roles in tumorigenesis. The anticancer functions of p53 include activating DNA repair enzymes, stopping the G1 to S phase transition by inducing p21 expression, and initiating apoptosis [6]. The *Ink4a/Arf* (*CDKN2A*) locus encodes tumor suppressors, p16^{Ink4a} and p14^{Arf} (p19^{Arf} in mouse). *p16*^{Ink4a} is a cyclin-dependent kinase inhibitor that binds to CDK4/6 to prevent interaction with cyclin D, effectively stopping the G1 to S phase transition [10]. Arf stabilizes p53 by promoting MDM2 degradation [11,12]. In addition, Arf possesses p53-independent functions such as cell cycle arrest, apoptosis, angiogenesis, and ribosomal RNA processing [13–17]. It has also been shown that Arf inhibits tumor cell colonization independent of p53 in a mouse model of PDAC metastasis [18].

Abbreviations: PACC, pancreatic acinar cell carcinoma; PDAC, pancreatic ductal adenocarcinoma; PanNET, pancreatic neuroendocrine tumor; H&E, hematoxylin and eosin stain

Address all correspondence to: Yi-Chieh Nancy Du, Department of Pathology and Laboratory Medicine, Weill Cornell Medicine, New York, NY 10065.
E-mail: nad2012@med.cornell.edu

[1] This work is partially supported by National Institutes of Health grants 2U01DK072473 and 1R21CA173348-01A1, Department of Defense grant W81XWH-13-1-0331, the Goldhirsh Foundation, and the President's Council of Cornell Women Affinito-Stewart Grant.
[2] The authors have declared that no competing interests exist.
Received 16 May 2016; Revised 12 August 2016; Accepted 15 August 2016

1476-5586
http://dx.doi.org/10.1016/j.neo.2016.08.003

Early studies found no *p53* mutations in PACCs by partial exon sequencing analysis [19,20], whereas *p53* loss of heterozygosity was observed in 50% and 70% of PACCs [20,21]. Because of advances in sequencing technology, recent studies report that *p53* loss by mutation and chromosomal loss is common in PACC [4,22–24]. Comprehensive genomic studies found that 13% to 23% of primary tumors had *TP53* point mutations or truncations [4,22] and 39% to 53% of primary tumors had *TP53* loss of heterozygosity [22,23]. In metastatic tumors, point mutations were identified in 31% and chromosomal deletions in 50%, suggesting that intact *p53* is a barrier to metastatic potential [23]. Emphasizing the clinical significance of *p53* status in PACC, copy number alterations and mutation with loss of heterozygosity were associated with shorter patient survival [23,24]. Although p53 mutations are rare in panNETs (<3%) [20], the p53 pathway is altered in approximately 70% of panNETs through aberrant activation of its negative regulators, including MDM2, MDM4, and WIP1 [6].

Loss of $p16^{Ink4a}$ in PACC occurs in lower frequency than loss of *p53*. Genomewide analyses identified homozygous deletion of $p16^{Ink4a}$ in 14% to 17% of PACCs [4,22]. In PanNETs, $p16^{Ink4a}$ is recognized as commonly altered and of prognostic value [10,25–27]. For PanNETs, Muscarella and colleagues analyzed 5 primary tumors and 5 metastatic PanNETs for genetic alteration of $p16^{Ink4a}$ and found that 9 of these 10 tumor specimens contain inactivating alteration of $p16^{Ink4a}$ [26]. With regard to clinical significance, low $p16^{Ink4a}$ levels in tumor tissue and promoter hypermethylation are negative prognostic factors of poor survival [10,27].

Although mouse model studies demonstrated that alterations in *p53* and *p16/p19* enable the malignant progression of PDAC [9,18,28], their contributions to PACC and PanNET are still not determined. To address the roles of *p53* and *p16/p19* in PACC and PanNET progression, we used mouse models that produce PACC and β-cell hyperplasia [29]. We previously showed that PyMT induction in *Pdx1*+ pancreatic progenitor cells results in β-cell hyperplasia in the majority of the mice and lethal PACC in <10% of mice, whereas *PyMT* induction in β cells results only in β-cell hyperplasia [29]. Although PyMT is not implicated in human cancer, it remains an important experimental tool because it stimulates signaling pathways important in human cancers: the mitogen-activated protein kinase, the phosphatidylinositol 3-kinase cascades, and the Hippo pathway [30–32]. Although the driver mutations for PACC and PanNET are unknown, activation of the mitogen-activated protein kinase pathway and phosphatidylinositol 3-kinase pathway is found in PACC and PanNET [4,33,34]. In this present study, we investigated the contribution of separate and combined *p53* and *p16/p19* loss to PACC and PanNET tumorigenesis in the mouse models. We find that in the context of PyMT expression in pancreatic *Pdx1*+ progenitor cells, *p53* loss results in highly malignant PACC, whereas *p16/p19* loss results in nonmetastatic PanNETs. However, concurrent loss of *p53* and *p16/p19* resembles loss of *p53,* suggesting that *p16/p19* loss has no additive effect to PACC progression promoted by loss of *p53* alone. In the context of PyMT expression in pancreatic β cells, *p53* loss results in nonmetastatic PanNETs, whereas *p16/p19* loss results in metastatic PanNETs. Concurrent loss of *p53* and *p16/p19* in pancreatic β-cells increases PanNET incidence compared with loss of either tumor suppressor alone.

Materials and Methods

Mouse Strains, Animal Husbandry, and Genotyping

Mice used in this study have a mixed genetic background. *Pdx1-tTA* knock-in mice were on an ICR genetic background [35]. *tet-o-PyMT-IRES-Luc* mice were generated on C57BL/6 genetic background [29] and were crossed to *p48-cre*; $p53^{lox/lox}$ and *p48-cre*; $p16/p19^{lox/lox}$ mice on an FVB/N background [36,37]. This study was carried out in strict accordance with the recommendations in the Guide for the Care and Use of Laboratory Animals of the National Institutes of Health. All mice were housed in accordance with institutional guidelines. Doxycycline rodent diets were obtained from Harlan-Teklad (Madison, WI). All procedures involving mice were approved by the Institutional Animal Care and Use Committee. Genotypes were determined by polymerase chain reaction using mouse ear DNA kept at −20°C or tumor DNA kept at −80°C, prepared through lysis in 0.05 M NaOH with 98°C incubation for 20 minutes and addition of 10 mM Tris–0.2 mM EDTA (pH 7.4). Cre recombinase excision of *p53* and *p16/p19* in tumor tissues was verified using primers for the recombined alleles.

Polymerase chain reaction primers were as follows: for PyMT: 5′-CTG CTACTGCACCCAGACAA-3′ and 5′-TCCGCCGTTTTGGATTA TAC-3′ (a 468-bp product); for tTA: 5′-GGACGAGCTCCACTTA GACG-3′ and 5′-AGGGCATCGGTAAACATCTG-3′ (a 200-bp product); for rtTA: 5′-GTGAAGTGGGTCCGCGTACAG-3′ and 5′-GTACTCGTCAATTCCAAGGGCATCG-3′(a 400-bp product); for unrecombined p16/p19 allele: 5′-CCTGACTATGGTAG TAAAGTGG-3′ and 5′-ACGTGTATGCCACCCTGACC-3′ (a 380-bp lox/lox, 280-bp WT product); for recombined p16/p19 allele: 5′-TTGGGAGGCACACTTTCTTGG-3′ (a 280-bp product); for unrecombined p53 allele: 5′-CACAAAAACAGGTTAAACCCAG-3′ and 5′-AGCACATAGGAGGCAGAGAC-3′ (a 370-bp lox/lox, 240-bp WT product); for recombined p53 allele: 5′-GAAGACAGAAAAGGG GAGGG-3′ (a 612-bp product); for p48-cre: 5′-GCGGTCTGGCAG TAAAAACTATC-3′ and 5′-GTGAAACAGCATTGCTGTCACTT-3′ (a 324-bp product).

Histology and Immunohistochemistry

Mice were sacrificed based on *in vivo* bioluminescent imaging (*PyMT* is linked to a *luciferase* reporter) when values in the region of pancreas exceeded 1e6 photons/sec, outward symptoms, and survival predictions. Mice found dead before sacrifice were dissected, and when possible, tumor burden, metastasis burden, and histology were examined. The tumor types were confirmed with immunohistochemistry using antibodies against chymotrypsin to identify acinar cells, synaptophysin to identify neuroendocrine cells, and keratin 17/19 to identify ductal cells.

Tissues from dissected mice were fixed in 10% buffered formalin overnight at room temperature and transferred to 70% ethanol for long-term storage. Tissues were sectioned into 5-μm slides and stained for hematoxylin and eosin (H&E) at Histoserv Inc. (Germantown, MD). Unstained sections were deparrafinized and rehydrated through a Clear-Rite/ethanol series. Histologic assessment was confirmed by immunohistochemistry with VECTASTAIN Elite ABC Kit (Vector Laboratories) performed based on the manufacturer's instructions. Primary antibodies used were anti-synaptophysin (1:100, Vector Labs, VP-S284) as a neuroendocrine marker and anti–keratin 17/19 (1:300, Cell Signaling, 3984) as a ductal marker. For automated staining of chymotrypsin, slides were pretreated with Protease 1 (Ventana) for 16 minutes and primary antibody, anti-human chymotrypsin antibody (Biodesign International, 1:3000), at 4°C overnight on the Ventana Benchmark platform according to manufacturer's instructions. The cutoff size used to differentiate between β-cell hyperplasia and PanNET is 1 mm in diameter [38].

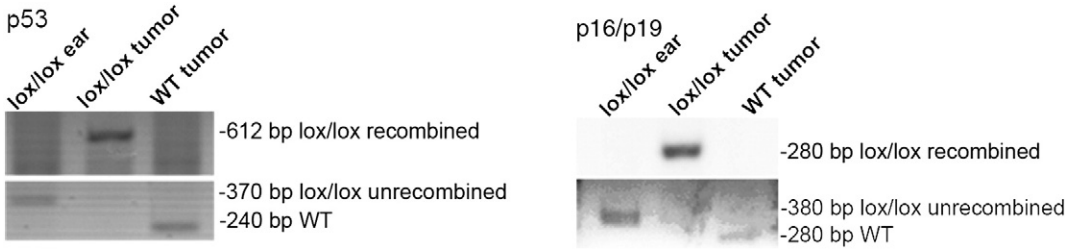

Figure 1. Analysis of primary tumor specimens from mice with p53 and p16/p19 mutants. Genotyping confirmed Cre-mediated recombination of the $p53^{lox/lox}$ and $p16/p19^{lox/lox}$ loci in tumor tissues. Genomic DNA from ears is used as control for unrecombined alleles.

Statistical Analysis

Survival was evaluated using the Kaplan-Meier method and statistically checked with the log-rank test using Prism (version 6.0f). Differences in tumor and metastasis incidence were examined by the χ^2 test. Differences in tumor burden were analyzed by *t* test. *P* value < .05 is considered as statistical significance.

Results

Generation of Mouse Lines

We have previously generated *Pdx1-tTA; tet-o-PyMT-IRES-Luc* (inducible *PyMT* in pancreatic progenitor cells) mouse model and described that PyMT expression in pancreatic progenitor cells results in β-cell hyperplasia in the majority of the mice or lethal PACC in <10% of mice [29]. To delete *p53* and *p16/p19* in the pancreatic cells of the PyMT mouse models, we crossed *Pdx1-tTA; tet-o-PyMT-IRES-Luc* to *p48-cre;* $p53^{lox/lox}$ mice and *p48-cre;* $p16/p19^{lox/lox}$ mice. The *p53* and *p16/p19* genomic loci were flanked with loxP sites [36,37] to allow generate nullizygous gene loci by Cre-mediated recombination. Cre recombinase was placed under a *p48* promoter, and recombination of *p53* and *p16/p19* in tumor tissue was confirmed using primers for the recombined alleles (Figure 1). Expression of Pdx1, a transcription factor necessary for pancreatic development, occurs at around E8.5 [39]. p48 is expressed slightly later than Pdx1 and is required to commit cells to a pancreatic fate [40].

Pdx1-tTA; tet-o-PyMT offers a baseline for comparison to tumor suppressor loss

Pdx1-tTA; tet-o-PyMT-IRES-Luc; p48-cre mice (n = 100, *Pdx1-tTA; tet-o-MT* for short) with mixed genetic background were used as the control group. Mice were not on doxycycline rodent diet, allowing PyMT to be induced in cells expressing the Pdx1 transcription factor. The tumor incidence of this genotype was 5% (5/100), and tumors were PACC (Table 1), in agreement with the previously reported tumor characteristics of the PyMT model in pure C57/BL6 genetic background [29]. Majority of the mice (95%) did not develop tumors, and only 2 of 100 mice (2%) had liver metastasis (Table 1). The survival of mice in this genotype, including those found dead, with or without tumors, is shown in Figure 2*A*. The phenotype of a normal pancreas and liver, commonly found in this control group, is shown in Figure 3*A*. Representative images of H&E staining of normal pancreatic tissue, β-cell hyperplasia, and PACC are presented in Figure 4, *A–C*, and normal liver histology is presented in Figure 6*A*.

p53 loss promotes PACC tumorigenesis and shortens survival

Pdx1-tTA; tet-o-PyMT-IRES-Luc; p48-cre; $p53^{lox/lox}$ mice (n = 20, *Pdx1-tTA; tet-o-MT;* $p53^{lox/lox}$ for short) have significantly shorter survival (P = .0002) and higher PACC incidence than *Pdx1-tTA; tet-o-MT* mice (20% vs 5%, P = .0025) (Table 1). Figure 3*B* is a representative image of a *Pdx1-tTA; tet-o-MT;* $p53^{lox/lox}$ mixed acinar-ductal carcinoma with a pancreatic tumor burden of 5463 cm^3 and multiple liver metastases. Immunohistochemistry of four tumors in this genotype revealed three mixed acinar-ductal carcinomas and one mixed acinar-neuroendocrine carcinoma (Table 1). Figure 5, *A–D* displays the immunohistochemical staining of a representative PACC tumor from the *Pdx1-tTA; tet-o-MT;* $p53^{lox/lox}$ genotype. The tumor is mixed with cells of ductal differentiation and no neuroendocrine components. Separate cells stained positive for ductal and acinar markers, but importantly, both cell types composed the same tumor, characterizing it as a mixed acinar-ductal carcinoma. The PACC tumor magnitudes were extensive (range: 1573-25,480 cm^3), and 4 of 4 (100%) mice that developed PACC had metastasis to the liver (Table 1). The histology of PACC liver metastasis is shown in Figure 6*B*. The majority of the tumor cells in *Pdx1-tTA; tet-o-MT;* $p53^{lox/lox}$ genotype were positive for chymotrypsin (an acinar marker) and negative for synaptophysin (a neuroendocrine marker) (Figure 5, *B* and *C*).

Table 1. Phenotypes of *p53* and *p16/p19* Loss in PACC and PanNET Mouse Models

	Genotype	Tumor Incidence (%)	*P* Value (χ^2) Tumor Incidence	PACC	PanNET	Metastasis (%)	*P* Value Survival
Pdx1-tTA; tet-o-MT; p48-cre	*p53WT; p16/p19WT*	5/100 (5%)		5 pure	0	2/5 (40%)	
	$p53^{lox/lox}$	4/20 (20%)	.020074	3A, 1 A/N	0	4/4 (100%)	.0002
	$p16/p19^{lox/lox}$	4/35 (11%)	.07102	1 pure	3	0/4 (0%)	.0025
	$p53^{lox/lox}$; $p16/p19^{lox/lox}$	4/12 (33%)	.000646	2A, 2U	0	4/4 (100%)	<.0001
RIP7-rtTA; tet-o-MT; p48-cre	*p53WT; p16/p19WT*	0/50 (0%)		0	0	0 (0%)	
	$p53^{lox/lox}$	2/12 (17%)	.003341	0	2	0/2 (0%)	.0129
	$p16/p19^{lox/lox}$	12/60 (20%)	.000807	0	12	5/12 (42%)	.3951
	$p53^{lox/lox}$; $p16/p19^{lox/lox}$	12/30 (40%)	.000002	0	12	4/12 (33%)	<.0001

A, mixed acinar ductal carcinoma; *A/N*, mixed acinar ductal neuroendocrine carcinoma; *U*, undetermined because of inability to stain necrotic tissue.

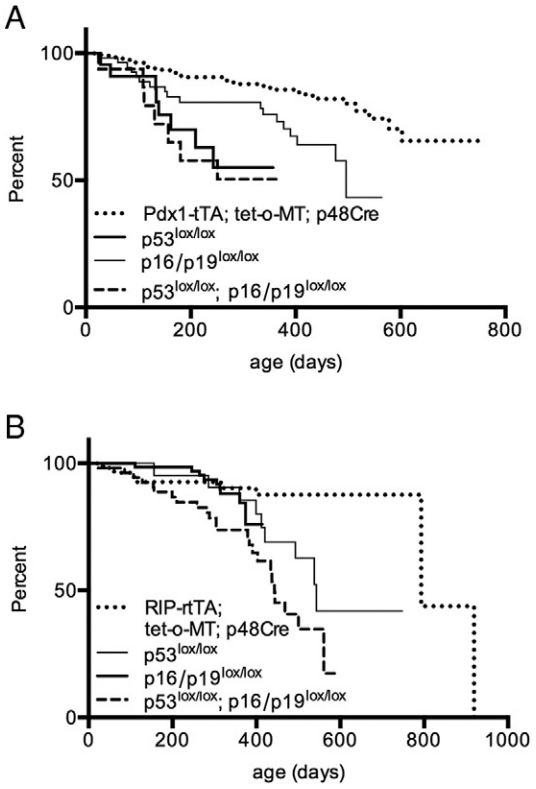

Figure 2. Kaplan-Meier curve displaying contribution of tumor suppressor loss to survival. (A) The survival of the three experimental groups with loss of tumor suppressor in pancreatic progenitors (*Pdx1-tTA; tet-o-MT; p48-cre; p53$^{lox/lox}$* mice, *Pdx1-tTA; tet-o-MT; p48-cre; p16/p19$^{lox/lox}$* mice, *Pdx1-tTA; tet-o-MT; p48-cre; p53$^{lox/lox}$; p16/p19$^{lox/lox}$* mice) was statistically shorter than the control *Pdx1-tTA; tet-o-MT; p48-cre* mice. Survival of *Pdx1-tTA; tet-o-MT; p48-cre; p53$^{lox/lox}$; p16/p19$^{lox/lox}$* was statistically different from that of *Pdx1-tTA; tet-o-MT; p48-cre; p16/p19$^{lox/lox}$* (P = .0449) but not statistically different from that of *Pdx1-tTA; tet-o-MT; p48-cre; p53$^{lox/lox}$*. (B) The survival of the three experimental groups with loss of tumor suppressor in pancreatic β cells (*RIP-rtTA; tet-o-MT; p48-cre; p53$^{lox/lox}$* mice, *RIP-rtTA; tet-o-MT; p48-cre; p16/p19$^{lox/lox}$* mice, *RIP-rtTA; tet-o-MT; p48-cre; p53$^{lox/lox}$; p16/p19$^{lox/lox}$* mice; all on dox) was statistically shorter than that of the control *RIP-rtTA; tet-o-MT; p48-cre* mice (on dox).

p16/p19 loss promotes PanNET tumorigenesis and shorts survival

Pdx1-tTA; tet-o-PyMT-IRES-Luc; p48-cre; p16/p19$^{lox/lox}$ mice (n = 35, *Pdx1-tTA; tet-o-MT; p16/p19$^{lox/lox}$* for short) have significantly shorter survival (P = .0025) and a slightly higher tumor incidence than control *Pdx1-tTA; tet-o-MT* mice (14% vs 5%, P = .0710) (Table 1, Figure 2*A*). The predominant tumor that developed was PanNET, apparent in 3 of 35 mice, and the average tumor burden was 43 cm^3 (range: 33-62 cm^3). Only 1 of 35 mice developed mixed acinar-ductal carcinoma (Table 1). None of the mice developed metastasis to the liver, suggesting that *p16/p19* loss in PyMT-expressing pancreatic progenitor cells is not sufficient to promote metastasis.

Concurrent loss of p53 and p16/p19 resembles loss of p53

Combined nullizygosity, *Pdx1-tTA; tet-o-PyMT-IRES-Luc; p48-cre; p53$^{lox/lox}$; p16/p19$^{lox/lox}$* (n = 12, *Pdx1-tTA; tet-o-MT; p53$^{lox/lox}$; p16/p19$^{lox/lox}$* for short), resulted in significantly shortened survival compared with *Pdx1-tTA; tet-o-MT* mice (P < .0001) (Table 1, Figure 2*A*). The tumor incidence was significantly higher than control mice (33% vs 5%, P = .0006) (Table 1). Survival was comparable to *Pdx1-tTA; tet-o-MT; p53$^{lox/lox}$* mice but was significantly shorter than *Pdx1-tTA; tet-o-MT; p16/p19$^{lox/lox}$* mice (P = .0449) (Figure 2*A*). PACC with liver metastasis occurred in four mice, but there was no PanNET incidence in this genotype (Table 1). The incidence of metastasis is similar to *Pdx1-tTA; tet-o-MT; p53$^{lox/lox}$* but differed significantly from *Pdx1-tTA; tet-o-MT; p16/p19$^{lox/lox}$* (P = .0289). The tumor latency of *Pdx1-tTA; tet-o-MT; p53$^{lox/lox}$; p16/p19$^{lox/lox}$* closely resembled *Pdx1-tTA; tet-o-MT; p53$^{lox/lox}$* (114 vs 119 days). Based on immunohistochemistry, two tumors were mixed acinar-ductal carcinomas and two were not determined because of the inability to stain necrotic tissue (Table 1). The average PACC tumor burden was 4447 cm^3 (range: 196-6240 cm^3). The tumor measuring 196 cm^3 was an acinar nodule in an 84-day-old mouse in early PACC tumor development. Taken together, the *Pdx1-tTA; tet-o-MT; p53$^{lox/lox}$; p16/p19$^{lox/lox}$* mice show similar survival, tumor incidence, phenotype, and metastasis to the *Pdx1-tTA; tet-o-MT; p53$^{lox/lox}$* mice, implying that *p16/p19* loss has no additive effect to *p53* loss.

p16/p19 loss, But Not p53 Loss, Results in Metastatic PanNETs in β-Cells

In addition to exploring the role of tumor suppressor loss in the *Pdx1-tTA; tet-o-MT* mouse model, we determined the contribution of *p53* and *p16/p19* loss to PanNET tumorigenesis in PyMT-expressing β-cells in the *RIP7-rtTA; tet-o-MT* mouse model. This model allows for elucidating a role for *p53* and *p16/p19* in PanNET tumorigenesis directly from pancreatic β cells.

The rat insulin promoter (RIP) is activated at around day E9.5 [41], and doxycycline is able to cross the placenta and to accumulate in the milk of lactating females [42] to interact with rtTA for PyMT induction. Mice with the control *RIP7-rtTA; tet-o-MT; p48-cre* genotype (n = 50) developed β-cell hyperplasia and had no PanNET development. However, PanNETs occurred in 17% of *RIP7-rtTA; tet-o-MT; p48-cre; p53$^{lox/lox}$* mice, 20% of *RIP7-rtTA; tet-o-MT; p48-cre; p16/p19$^{lox/lox}$* mice, and 40% of *RIP7-rtTA; tet-o-MT; p48-cre; p53$^{lox/lox}$; p16/p19$^{lox/lox}$* mice (Table 1). Liver metastases were not present in *RIP7-rtTA; tet-o-MT; p53$^{lox/lox}$* mice but occurred in 5 of 60 (8%) of *RIP7-rtTA; tet-o-MT; p16/p19$^{lox/lox}$* mice and 4 of 30 (13%) of *RIP7-rtTA; tet-o-MT; p53$^{lox/lox}$; p16/p19$^{lox/lox}$* mice (Table 1). The absence of metastases from *RIP7-rtTA; tet-o-MT; p53$^{lox/lox}$* further supports that *p16/p19* loss is more relevant in PanNET progression than *p53* loss. Figure 3*C* represents a PanNET and liver metastases that developed in *RIP7-rtTA; tet-o-MT; p16/p19$^{lox/lox}$*. Figure 5, *E–H* presents the H&E and immunohistochemical staining of a representative PanNET from the *RIP7-rtTA; tet-o-MT; p16/p19$^{lox/lox}$* genotype. Figure 6*C* displays the histology of a typical PanNET liver metastasis.

Discussion

We investigate the functions of p53 and *p16/p19* tumor suppressor loss in PACC and PanNET in mouse models. This is the first study, to our knowledge, that shows a causal role of *p53* loss in producing short-latency, metastatic PACC without neuroendocrine feature. We found that *Pdx1-tTA; tet-o-MT; p48-cre; p53$^{lox/lox}$* mice demonstrated shorter survival, increased tumor incidence, and increased metastasis as compared with the control *Pdx1-tTA; tet-o-MT; p48-cre* mice, emphasizing that *p53* plays an important role in PACC progression. On the other hand, *p16/p19* loss is not sufficient to advance PACC progression. *Pdx1-tTA; tet-o-MT; p48-cre; p16/p19$^{lox/lox}$* had no

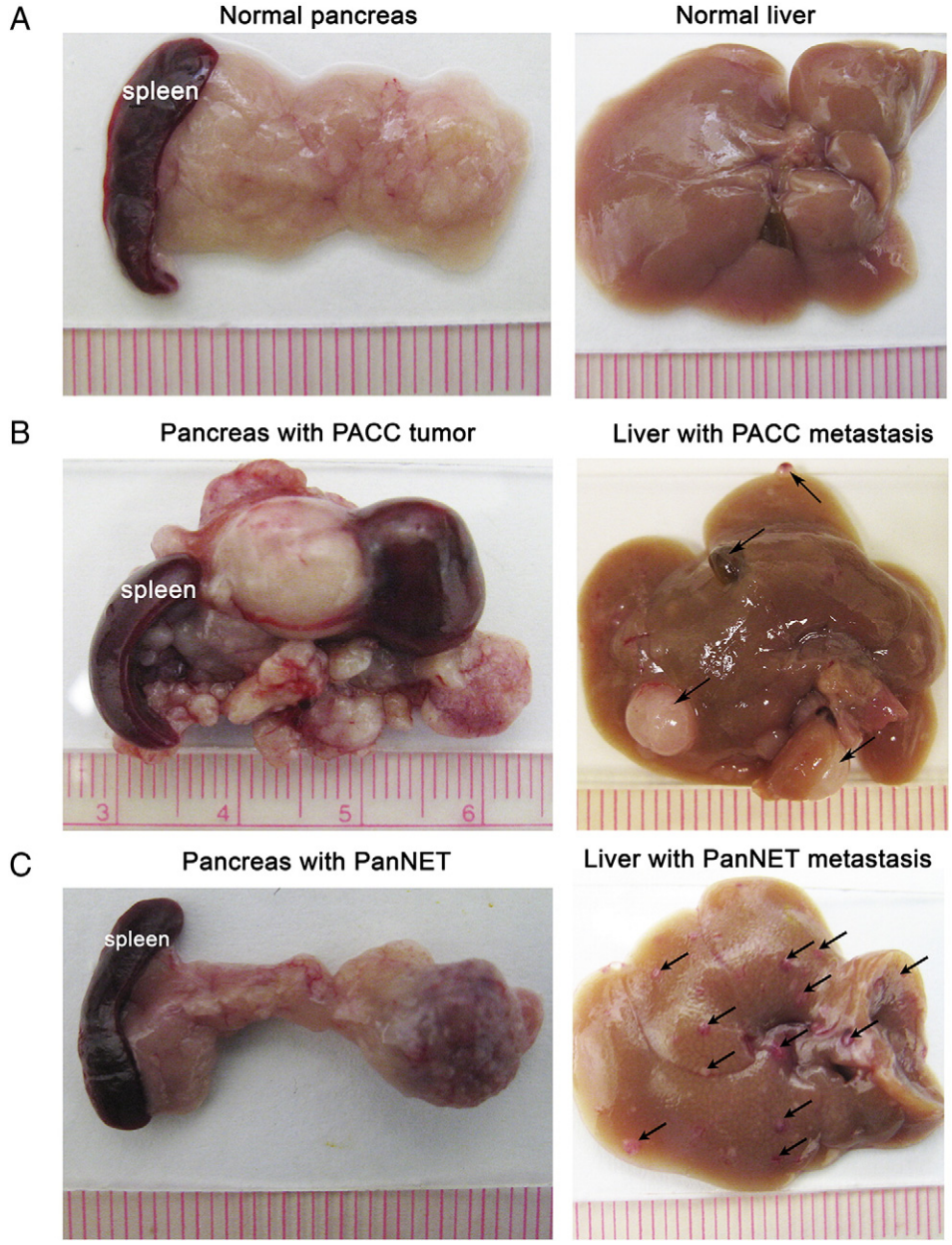

Figure 3. Macroscopic phenotypic changes of the pancreas and liver. Gross photograph of (A) normal pancreas and liver. (B) PACC tumor and liver metastases from *Pdx1-tTA; tet-o-MT; p48-cre; p53*$^{lox/lox}$ genotype. (C) PanNET and liver metastases indicated by black arrows in the *RIP7-rtTA; tet-o-MT; p48-cre; p16/p19*$^{lox/lox}$ genotype. *Pdx1-tTA; tet-o-MT; p48-cre; p16/p19*$^{lox/lox}$ mice develop PanNETs but not metastases. Scale: mm.

increase in PACC incidence over the control characteristics of the *Pdx1-tTA; tet-o-MT; p48-cre* mice but did have shortened survival due to the development of PanNETs. Additionally, there were no differences in tumor incidence, burden, metastasis, or survival between concurrent loss of both *p53* and *p16/p19* and loss of *p53* alone in the *Pdx1-tTA; tet-o-MT* model, suggesting that there is no additive effect of *p16/p19* loss to PACC promoted by *p53* loss.

Two elegant studies by Lewis et al. [43] and Morton et al. [44] used an RCASBP-tva system to deliver *PyMT* into elastase-*tva* mice postnatally. The elastase promoter has been used in transgenic mice with the intent of expressing genes specifically in the acinar cells of the pancreas. In this elastase-*tva* mouse model, RCAS-*PyMT* induces only microscopic pancreatic intraepithelial neoplasia in wild-type tumor suppressor background [43]. RCAS-*PyMT*–induced acinar cell carcinomas in *p53* null background [44] are uniformly positive for both chymotrypsin (an acinar marker) and synaptophysin (a neuroendocrine marker). The feature is similar to human mixed acinar neuroendocrine carcinoma [45]. In contrast, the majority of acinar tumors in our *Pdx1-tTA; tet-o-MT; p48-cre* mice or *Pdx1-tTA; tet-o-MT; p48-cre; p53*$^{lox/lox}$ mice expressed chymotrypsin but did not express synaptophysin, and therefore, this PACC tumor type described here is different from RCAS-*PyMT* tumors in elastase-*tva* mice. We did not see an additive effect of combined *p53* and *p16/19* deletion for this acinar tumor type in our mouse model, which is different from the RCAS-*PyMT* mouse model [44]. Moreover, RCAS-*PyMT*–induced acinar cell carcinomas in *p16/p19* null

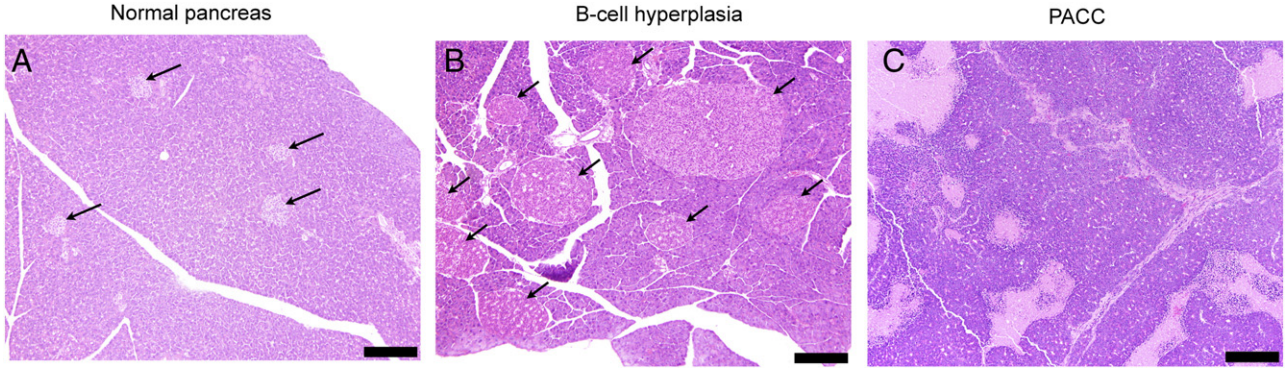

Figure 4. Histologic features of the *Pdx1-tTA; tet-o-MT; p48-cre* mouse model. H&E of (A) normal pancreas, (B) β-cell hyperplasia, and (C) pure PACC at 10× magnification. Arrows point to normal-sized islets in (A) and β-cell hyperplasia in (B). Bar indicates 200 μm.

background [43] are also uniformly positive for both chymotrypsin and synaptophysin. However, loss of *p16/p19* in *Pdx1-tTA; tet-o-MT; p48-cre; p16/p19*$^{lox/lox}$ mice promoted PanNET, which is negative for chymotrypsin (Figure 5*F*). Altogether, the differences in tumor types may reflect cell of origin differences in our tet-inducible PyMT model and the RCAS-*PyMT*/elastase-*tva* model.

In addition, the tumor formation is slower and tumor incidence is lower in *Pdx1-tTA; tet-o-MT; p48-cre; p53*$^{lox/lox}$ mice than in RCAS-*PyMT* infected elastase-*tva* mice in *p53* null background [44]. This could be a consequence of the low Pdx1 expression in acinar cells in adult pancreas and the timing of PyMT expression during pancreatic development in *Pdx1-tTA; tet-o-MT; p48-cre; p53*$^{lox/lox}$ mice.

We did not observe PanNETs in *Pdx1-tTA; tet-o-MT; p48-cre; p53*$^{lox/lox}$ mice. This is likely due to the rapidity of PACC tumorigenesis, which caused the lethality of the mice. By using another mouse model, *RIP7-rtTA; tet-o-MT*, which developed β-cell hyperplasia, *p53* loss resulted in small nodular PanNETs without metastases, indicating that *p53* loss can promote neuroendocrine tumorigenesis in β-cells but is not a barrier to metastatic potential.

Our study also establishes the causal role of *p16/p19* loss in PanNET tumorigenesis but not in PACC tumorigenesis as evidenced by the development of only PanNETs in *Pdx1-tTA; tet-o-MT; p48-cre; p16/p19*$^{lox/lox}$ mice. Loss of *p16/p19* in *Pdx1*+ pancreatic progenitor cells enhanced the tumorigenesis of specifically the β-cell lineage and not the acinar lineage. Interestingly, *p16/p19* loss in the *RIP7-rtTA* model promoted liver metastases of PanNET, whereas its loss in the *Pdx1-tTA* model did not result in metastasis of PanNET. The differences could be due to 1) the expression levels of rtTA and tTA driven by RIP promoter and Pdx1 promoter or 2) the order of PyMT expression and the *p16/p19* loss.

In this study, we demonstrate that with PyMT expression starting from pancreatic *Pdx1*+ progenitor cells, *p53* loss has a causal role in PACC tumorigenesis and metastasis, whereas *p16/p19* loss promotes long-latency, nonmetastatic PanNETs. *p53* loss and *p16/p19* loss do not have cooperative roles in PACC tumorigenesis. In PyMT-expressing β cells, both tumor suppressors play critical and cooperative roles in PanNET tumorigenesis.

Acknowledgements

The authors thank Leigh Selesner, Bu Jung Kim, Soyoung Choi, Samantha Li, Megan Wong, and George Zhang of the Du lab; Zhengming Chen for statistical advice; Danny Huang for mouse database design; and Irina Linkov for chymotrypsin staining. This

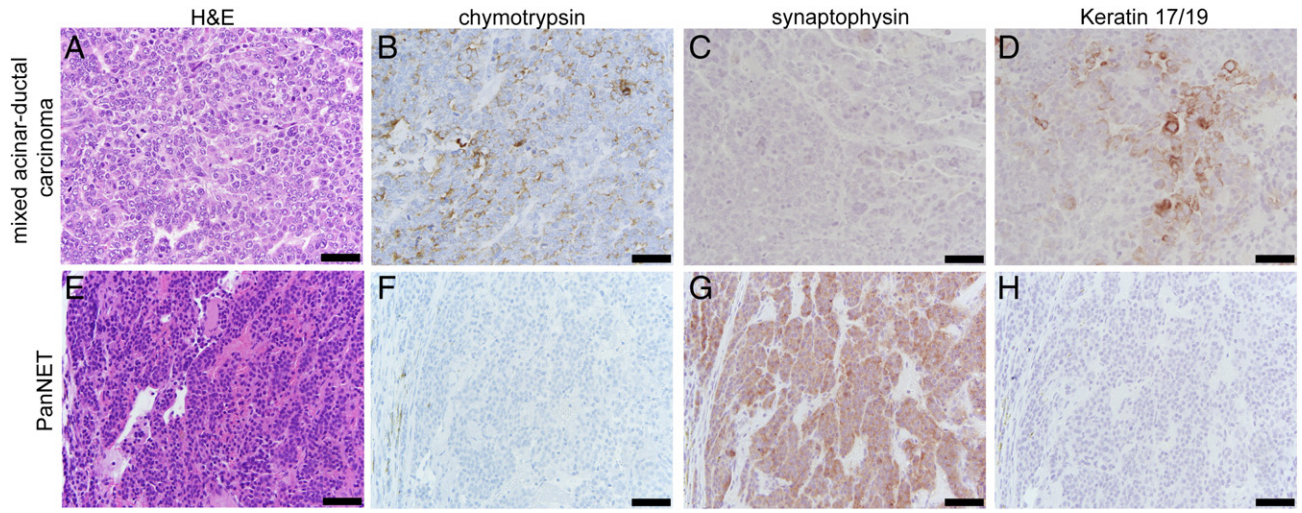

Figure 5. Tumor type determination with immunohistochemistry. PACC mixed with ductal components from the *Pdx1-tTA; tet-o-MT; p48-cre; p53*$^{lox/lox}$ mice at 40× magnification stained for (A) H&E, (B) chymotrypsin (+), (C) synaptophysin (−), and (D) keratin 17/19 (+). PanNET tissue from the *Pdx1-tTA; tet-o-MT; p48-cre; p16/p19*$^{lox/lox}$ mice at 40× magnification stained for (E) H&E, (F) chymotrypsin (−), (G) synaptophysin (+), and (H) keratin 17/19 (−). Bars indicate 50 μm.

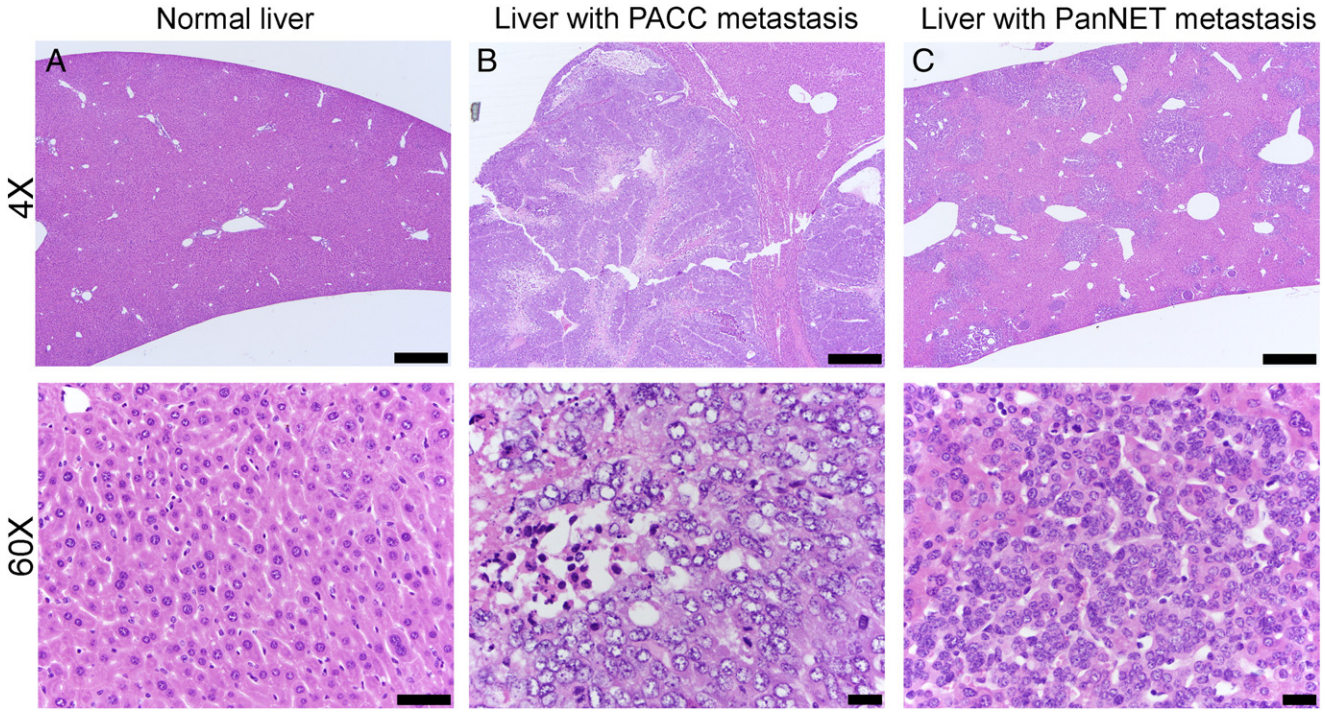

Figure 6. Microscopic phenotypic differences in liver histology. H&E staining of (A) normal liver from the *Pdx1-tTA; tet-o-MT; p48-cre* genotype, (B) liver with PACC metastases from the *Pdx1-tTA; tet-o-MT; p48-cre; p53$^{lox/lox}$* genotype, and (C) liver with PanNET metastases from the *RIP7-rtTA; tet-o-MT; p48-cre; p16/p19$^{lox/lox}$* genotype. In the upper panel (4× magnification), bars indicate 500 μm. In the lower panel (60× magnification), bars indicate 50, 20, and 20 μm (left to right).

work is partially supported by National Institutes of Health grants 2U01DK072473 and 1R21CA173348-01A1, Department of Defense grant W81XWH-13-1-0331, the Goldhirsh Foundation, and the President's Council of Cornell Women Affinito-Stewart Grant. Special thanks for the Opportunities Fund of Macaulay Honors College at CUNY Hunter to S.A. and S.P. The authors have declared that no conflicts of interest exist.

References

[1] La Rosa S, Sessa F, and Capella C (2015). Acinar cell carcinoma of the pancreas: overview of clinicopathologic features and insights into the molecular pathology. *Front Med (Lausanne)* **2**, 41.

[2] Zhou C, Zhang J, Zheng Y, and Zhu Z (2012). Pancreatic neuroendocrine tumors: a comprehensive review. *Int J Cancer* **131**, 1013–1022.

[3] Reid MD, Bagci P, and Adsay NV (2013). Histopathologic assessment of pancreatic cancer: does one size fit all? *J Surg Oncol* **107**, 67–77.

[4] Chmielecki J, Hutchinson KE, Frampton GM, Chalmers ZR, Johnson A, Shi C, Elvin J, Ali SM, Ross JS, and Basturk O, et al (2014). Comprehensive genomic profiling of pancreatic acinar cell carcinomas identifies recurrent RAF fusions and frequent inactivation of DNA repair genes. *Cancer Discov* **4**, 1398–1405.

[5] Wood LD and Hruban RH (2015). Genomic landscapes of pancreatic neoplasia. *J Pathol Transl Med* **49**, 13–22.

[6] Hu W, Feng Z, Modica I, Klimstra DS, Song L, Allen PJ, Brennan MF, Levine AJ, and Tang LH (2010). Gene amplifications in well-differentiated pancreatic neuroendocrine tumors inactivate the p53 pathway. *Genes Cancer* **1**, 360–368.

[7] Bergmann F, Aulmann S, Sipos B, Kloor M, von Heydebreck A, Schweipert J, Harjung A, Mayer P, Hartwig W, and Moldenhauer G, et al (2014). Acinar cell carcinomas of the pancreas: a molecular analysis in a series of 57 cases. *Virchows Arch* **465**, 661–672.

[8] La Rosa S, Adsay V, Albarello L, Asioli S, Casnedi S, Franzi F, Marando A, Notohara K, Sessa F, and Vanoli A, et al (2012). Clinicopathologic study of 62 acinar cell carcinomas of the pancreas: insights into the morphology and immunophenotype and search for prognostic markers. *Am J Surg Pathol* **36**, 1782–1795.

[9] Bardeesy N, Aguirre AJ, Chu GC, Cheng KH, Lopez LV, Hezel AF, Feng B, Brennan C, Weissleder R, and Mahmood U, et al (2006). Both p16(Ink4a) and the p19(Arf)-p53 pathway constrain progression of pancreatic adenocarcinoma in the mouse. *Proc Natl Acad Sci U S A* **103**, 5947–5952.

[10] Liu S, Chang Y, Ma J, Li X, Li X, Fan J, Huang R, Duan G, and Sun X (2013). Prognostic impact of p16 and p21 on gastroenteropancreatic neuroendocrine tumors. *Oncol Lett* **6**, 1641–1645.

[11] Pomerantz J, Schreiber-Agus N, Liegeois NJ, Silverman A, Alland L, Chin L, Potes J, Chen K, Orlow I, and Lee HW, et al (1998). The Ink4a tumor suppressor gene product, p19Arf, interacts with MDM2 and neutralizes MDM2's inhibition of p53. *Cell* **92**, 713–723.

[12] Zhang Y, Xiong Y, and Yarbrough WG (1998). ARF promotes MDM2 degradation and stabilizes p53: ARF-INK4a locus deletion impairs both the Rb and p53 tumor suppression pathways. *Cell* **92**, 725–734.

[13] Ulanet DB and Hanahan D (2010). Loss of p19(Arf) facilitates the angiogenic switch and tumor initiation in a multi-stage cancer model via p53-dependent and independent mechanisms. *PLoS One* **5**e12454.

[14] Sugimoto M, Kuo ML, Roussel MF, and Sherr CJ (2003). Nucleolar Arf tumor suppressor inhibits ribosomal RNA processing. *Mol Cell* **11**, 415–424.

[15] Kuo ML, Duncavage EJ, Mathew R, den Besten W, Pei D, Naeve D, Yamamoto T, Cheng C, Sherr CJ, and Roussel MF (2003). Arf induces p53-dependent and -independent antiproliferative genes. *Cancer Res* **63**, 1046–1053.

[16] Itahana K, Bhat KP, Jin A, Itahana Y, Hawke D, Kobayashi R, and Zhang Y (2003). Tumor suppressor ARF degrades B23, a nucleolar protein involved in ribosome biogenesis and cell proliferation. *Mol Cell* **12**, 1151–1164.

[17] Eymin B, Leduc C, Coll JL, Brambilla E, and Gazzeri S (2003). p14ARF induces G2 arrest and apoptosis independently of p53 leading to regression of tumours established in nude mice. *Oncogene* **22**, 1822–1835.

[18] Muniz VP, Barnes JM, Paliwal S, Zhang X, Tang X, Chen S, Zamba KD, Cullen JJ, Meyerholz DK, and Meyers S, et al (2011). The ARF tumor suppressor inhibits tumor cell colonization independent of p53 in a novel mouse model of pancreatic ductal adenocarcinoma metastasis. *Mol Cancer Res* **9**, 867–877.

[19] Pellegata NS, Sessa F, Renault B, Bonato M, Leone BE, Solcia E, and Ranzani GN (1994). K-ras and p53 gene mutations in pancreatic cancer: ductal and nonductal tumors progress through different genetic lesions. *Cancer Res* **54**, 1556–1560.

[20] Moore PS, Orlandini S, Zamboni G, Capelli P, Rigaud G, Falconi M, Bassi C, Lemoine NR, and Scarpa A (2001). Pancreatic tumours: molecular pathways implicated in ductal cancer are involved in ampullary but not in exocrine nonductal or endocrine tumorigenesis. *Br J Cancer* **84**, 253–262.

[21] Rigaud G, Moore PS, Zamboni G, Orlandini S, Taruscio D, Paradisi S, Lemoine NR, Kloppel G, and Scarpa A (2000). Allelotype of pancreatic acinar cell carcinoma. *Int J Cancer* **88**, 772–777.

[22] Jiao Y, Yonescu R, Offerhaus GJ, Klimstra DS, Maitra A, Eshleman JR, Herman JG, Poh W, Pelosof L, and Wolfgang CL, et al (2014). Whole-exome sequencing of pancreatic neoplasms with acinar differentiation. *J Pathol* **232**, 428–435.

[23] La Rosa S, Bernasconi B, Frattini M, Tibiletti MG, Molinari F, Furlan D, Sahnane N, Vanoli A, Albarello L, and Zhang L, et al (2016). TP53 alterations in pancreatic acinar cell carcinoma: new insights into the molecular pathology of this rare cancer. *Virchows Arch* **468**, 286–296.

[24] Furlan D, Sahnane N, Bernasconi B, Frattini M, Tibiletti MG, Molinari F, Marando A, Zhang L, Vanoli A, and Casnedi S, et al (2014). APC alterations are frequently involved in the pathogenesis of acinar cell carcinoma of the pancreas, mainly through gene loss and promoter hypermethylation. *Virchows Arch* **464**, 553–564.

[25] Simon B and Lubomierski N (2004). Implication of the INK4a/ARF locus in gastroenteropancreatic neuroendocrine tumorigenesis. *Ann N Y Acad Sci* **1014**, 284–299.

[26] Muscarella P, Melvin WS, Fisher WE, Foor J, Ellison EC, Herman JG, Schirmer WJ, Hitchcock CL, DeYoung BR, and Weghorst CM (1998). Genetic alterations in gastrinomas and nonfunctioning pancreatic neuroendocrine tumors: an analysis of p16/MTS1 tumor suppressor gene inactivation. *Cancer Res* **58**, 237–240.

[27] House MG, Herman JG, Guo MZ, Hooker CM, Schulick RD, Lillemoe KD, Cameron JL, Hruban RH, Maitra A, and Yeo CJ (2003). Aberrant hypermethylation of tumor suppressor genes in pancreatic endocrine neoplasms. *Ann Surg* **238**, 423–431 [discussion 431-422].

[28] Hingorani SR, Wang L, Multani AS, Combs C, Deramaudt TB, Hruban RH, Rustgi AK, Chang S, and Tuveson DA (2005). Trp53R172H and KrasG12D cooperate to promote chromosomal instability and widely metastatic pancreatic ductal adenocarcinoma in mice. *Cancer Cell* **7**, 469–483.

[29] Du YC, Klimstra DS, and Varmus H (2009). Activation of PyMT in beta cells induces irreversible hyperplasia, but oncogene-dependent acinar cell carcinomas when activated in pancreatic progenitors. *PLoS One* **4**e6932.

[30] Dilworth SM (2002). Polyoma virus middle T antigen and its role in identifying cancer-related molecules. *Nat Rev Cancer* **2**, 951–956.

[31] Shanzer M, Ricardo-Lax I, Keshet R, Reuven N, and Shaul Y (2015). The polyomavirus middle T-antigen oncogene activates the Hippo pathway tumor suppressor Lats in a Src-dependent manner. *Oncogene* **34**, 4190–4198.

[32] Courtneidge SA and Smith AE (1983). Polyoma virus transforming protein associates with the product of the c-src cellular gene. *Nature* **303**, 435–439.

[33] Jiao Y, Shi C, Edil BH, de Wilde RF, Klimstra DS, Maitra A, Schulick RD, Tang LH, Wolfgang CL, and Choti MA, et al (2011). DAXX/ATRX, MEN1, and mTOR pathway genes are frequently altered in pancreatic neuroendocrine tumors. *Science* **331**, 1199–1203.

[34] Capurso G, Di Florio A, Sette C, and Delle Fave G (2013). Signalling pathways passing Src in pancreatic endocrine tumours: relevance for possible combined targeted therapies. *Neuroendocrinology* **97**, 67–73.

[35] Holland AM, Hale MA, Kagami H, Hammer RE, and MacDonald RJ (2002). Experimental control of pancreatic development and maintenance. *Proc Natl Acad Sci U S A* **99**, 12236–12241.

[36] Krimpenfort P, Quon KC, Mooi WJ, Loonstra A, and Berns A (2001). Loss of p16Ink4a confers susceptibility to metastatic melanoma in mice. *Nature* **413**, 83–86.

[37] Jonkers J, Meuwissen R, van der Gulden H, Peterse H, van der Valk M, and Berns A (2001). Synergistic tumor suppressor activity of BRCA2 and p53 in a conditional mouse model for breast cancer. *Nat Genet* **29**, 418–425.

[38] Lopez T and Hanahan D (2002). Elevated levels of IGF-1 receptor convey invasive and metastatic capability in a mouse model of pancreatic islet tumorigenesis. *Cancer Cell* **1**, 339–353.

[39] Offield MF, Jetton TL, Labosky PA, Ray M, Stein RW, Magnuson MA, Hogan BL, and Wright CV (1996). PDX-1 is required for pancreatic outgrowth and differentiation of the rostral duodenum. *Development* **122**, 983–995.

[40] Kawaguchi Y, Cooper B, Gannon M, Ray M, MacDonald RJ, and Wright CV (2002). The role of the transcriptional regulator Ptf1a in converting intestinal to pancreatic progenitors. *Nat Genet* **32**, 128–134.

[41] Gittes GK and Rutter WJ (1992). Onset of cell-specific gene expression in the developing mouse pancreas. *Proc Natl Acad Sci U S A* **89**, 1128–1132.

[42] Passman RS and Fishman GI (1994). Regulated expression of foreign genes in vivo after germline transfer. *J Clin Invest* **94**, 2421–2425.

[43] Lewis BC, Klimstra DS, and Varmus HE (2003). The c-myc and PyMT oncogenes induce different tumor types in a somatic mouse model for pancreatic cancer. *Genes Dev* **17**, 3127–3138.

[44] Morton JP, Klimstra DS, Mongeau ME, and Lewis BC (2008). Trp53 deletion stimulates the formation of metastatic pancreatic tumors. *Am J Pathol* **172**, 1081–1087.

[45] Sigel CS and Klimstra DS (2013). Cytomorphologic and immunophenotypical features of acinar cell neoplasms of the pancreas. *Cancer Cytopathol* **121**, 459–470.